Environmentally Friendly Packaging Materials Based on Thermoplastic Starch

V. Ocelić Bulatović,[a,*] L. Mandić,[a] A. Turković,[a] D. Kučić Grgić,[a] A. Jozinović,[b] R. Zovko,[a] and E. Govorčin Bajsić[a]

[a]University of Zagreb, Faculty of Chemical Engineering and Technology, Marulićev trg 19, HR-10000 Zagreb, Croatia

[b]Josip Juraj Strossmayer University of Osijek, Faculty of Food Technology Osijek, F. Kuhača 20, HR-31000 Osijek, Croatia

https://doi.org/10.15255/CABEQ.2018.1548

Original scientific paper
Received: November 29, 2018
Accepted: September 6, 2019

Low-density polyethylene (LDPE) is extensively used as packaging material, and as such has a short service life, but long environmental persistence. The alternative to reducing the impact of LDPE as packaging material on the environment is to blend it with carbohydrate-based polymers, like starch. Therefore, the focus of this investigation was to prepare bio-based blends of LDPE and thermoplastic starch (TPS) containing different amounts of TPS using a Brabender kneading chamber. Due to incompatibility of LDPE/TPS blends, a styrene–ethylene/butylene–styrene block copolymer, grafted with maleic anhydride (SEBS-g-MA) containing 2 mol % anhydride groups, was added as a compatibilizer. The effect of the biodegradable, hydrophilic TPS, its content, and the incorporation of the compatibilizer on the properties of LDPE/TPS blends were analysed. The characterization was performed by means of thermogravimetric analysis (TG), differential scanning calorimetry (DSC), scanning electron microscopy (SEM), and water absorption (WA). Based on the results of the morphological structure, a good dispersion of the TPS phase in LDPE matrix was obtained with the incorporation of compatibilizer, which resulted in better thermal and barrier properties of these materials.

Keywords:

low-density polyethylene, thermoplastic starch, compatibilizer, morphology, thermal and barrier properties

Introduction

The importance of synthetic polymers has continuously increased worldwide, and they are still one of the most commonly used materials in the world.[1–6] The increasing trend in the use of synthetic polymer materials is attributed to their specific properties, such as low price, excellent mechanical and barrier properties, lightweight nature, resistance to physical aging and biological processes in the environment.[3–7] Today, it is difficult to imagine life without plastics, which are mostly derived from crude oils and natural gas. Among the various synthetic polymers, polyethylene, polypropylene, and polystyrene are used mostly for plastic packaging, in the biomedical field and in agriculture.[8,9] More than 40 % of the synthetic polymer materials are used as plastic packaging.[3–5,9]

Polyethylene, especially low-density polyethylene (LDPE), is one of the most dominant plastic packaging materials. The main problem with plastic packaging is that it is thrown uncontrollably into the environment after use. Most of the packaging is used once, resulting in the daily formation of large amounts of plastic packaging waste. Precisely this problem of accumulating packaging waste encourages us to develop and improve waste management awareness. However, synthetic polymers are petroleum-based plastics, which are not biodegradable and totally recyclable, and cause serious environmental and economic problems related to the increasing volume of plastic waste and the consumption of non-renewable resources arising from plastic production.[2–6,10–12]

Therefore, emphasis is put on the development of biodegradable materials and renewable polymer sources subjected to controlled biodegradation in the presence of natural organisms as the most desirable way to decompose materials.[13–16] However, the widespread use of biodegradable polymeric materials in comparison to synthetic polymers is still limited, due to their poor properties and difficult processing, and is still the subject of much research.[10–12,16,17]

*Corresponding author: Email: vocelicbu@simet.hr

In order to reduce the amount of applications of synthetic polymer materials while retaining the quality and low price of packaging, blending of synthetic and biodegradable polymers is an ideal solution. The blended materials offer a wide variety of mechanical, physical, optical, and barrier properties. Very often, they have better properties than the individual components. The blending of synthetic polymers with biodegradable polymers, such as thermoplastic starch, makes bio-based blends.[8,10–12]

From an ecological point of view, it is important that the obtained bio-based materials be decomposable and/or compostable, that there is a sufficient amount of biopolymer in the blend, and that the microorganisms in the environment for waste disposal prefer and consume that particular biopolymer. Furthermore, not only will the biopolymer be consumed, but the degradation rate of the synthetic polymer will increase as a result of the enhancing oxidation chain reactions. Therefore, the use of these bio-based blends in daily life will reduce the amount of plastic waste, as well as reduce the use of petroleum-based plastic materials.

Starch, as a biodegradable polymer, has great potential in application, due to its natural biodegradability in a wide range of environments, low cost, non-toxicity, and availability.[11–14,18–20] Industrial starch is derived from renewable resources, such as corn, tapioca, wheat, some potatoes, and rice.[13,14,16] From a chemical point of view, starch consists of two polymers, essential linear amylose (up to 25 %), and highly branched amylopectin (up to 75 %). By nature, starch is not a typical thermoplastic polymeric material.[13–16] Since the melting temperature (T_m) of pure dry starch is between 220–240 °C, and its degradation temperature is about 220 °C, natural starch must be modified so that it can be processed by classical technologies used in the plastic processing industries, like extrusion, injection moulding, compression, etc.[13] One of the most known natural starch modification processes is plasticizing by adding a plasticizer (water, glycerol, sorbitol, etc.) with simultaneous action of temperature and shear. The transformation of natural starch into thermoplastic-like material is called gelatinization, and the material obtained in this way is referred to as thermoplastic starch (TPS).[13–20] The gelatinization of starch results in the destruction of the crystalline structure of native starch, mainly amylopectin, so that a completely amorphous polymer is obtained.[13,21–23] On the other hand, glycerol is the most popular plasticizer for TPS contributing to an improvement in the degree of crystallinity of blends.[9,24,25] Plasticizers exchange the intermolecular bonds between starch polymer chains and promote conformational changes resulting in enhanced flexibility.[13,26] Both the glass transition and processing temperature of the material decrease, thus enabling the melt processing of heat-sensitive polymers at lower temperatures.[13,27] The nature and concentration of the plasticizer strongly influence the rheological and mechanical properties of TPS. Neat starch has a high glass transition temperature, and its relatively large modulus and strength is accompanied by poor deformability and impact resistance, due to the limited conformational mobility of its stiff chains.[13–16,28]

The blending of synthetic polymers with thermoplastic starch is a significant way to overcome the limitations of a particular material, namely to improve the weak mechanical and thermal properties of TPS, and on the other hand, the addition of TPS improves the biodegradability of such blends.[2,6–10,24] The aim is to obtain environmentally friendly and economical materials. The most important drawback in designing and developing bio-based polymer blends with TPS is the chemical incompatibility between hydrophilic TPS and the hydrophobic low-density polyethylene.[6,7,8,24] Incompatibility at the interface results in reduced adhesion, which causes phase separation and weak properties of such materials. Therefore, the addition of a compatibilizer is an essential step in developing such blends. The role of the compatibilizer is to reduce the interfacial tension between the polymers, in order to achieve fine dispersion of one phase to the other, leading to phase separation reduction, intermediate tension, and improving the adhesion on the interphase, which results in improved processing and application properties of the final material.[8,10,26,29–31]

The aim of this paper was to investigate and gain scientific understanding of the influence of a styrene–ethylene/butylene–styrene block copolymer, grafted with maleic anhydride (SEBS-g-MA), on the miscibility of low-density polyethylene (LDPE) and thermoplastic starch, in order to obtain a relationship between the composition of the blend, type, and proportion of the individual phases in the blends. In addition, the compatibility effect on the morphological structure, thermal and barrier properties important for the application of LDPE/TPS blends as packing materials, were also examined.

Experimental

Materials

Low-density polyethylene (LDPE), Dow 150 E, with a melt flow index 0.25 g/10 min at 190 °C, was purchased from Dow Chemical Company. The native wheat starch (12.20 % moisture) ‘‘Srpanjka” (harvest 2008) was obtained from the Agricultural Institute, Osijek, Croatia. The content of amylose in

isolated native wheat starch was 22.49±2.01 wt%. The plasticizer, glycerol, was purchased from Gram Mol, Zagreb, Croatia. Styrene–ethylene/butylene–styrene block copolymer, grafted with maleic anhydride (SEBS-g-MA), Kraton FG 1901X, was fabricated by the Shell Chemicals Company, USA, and was used in this study as a compatibilizer. SEBS-g-MA as a three-block polymer, grafted with 2 wt% maleic anhydride. According to the manufacturer, the styrene/ethylene-butylene ratio is 28/72.

Preparations

Thermoplastic starch (TPS) was prepared by mixing native wheat starch in powder form (Fig. 1 (a)) with liquid glycerol added as a plasticizer. The ratio of starch to glycerol was 60/40. The TPS was extruded in a laboratory single-screw extruder (Model 19/20DN; Brabender GmbH, Germany). The temperature profile in the first (dosing), second (compression), and third (ejection) zone was 100, 100, and 130 °C, respectively, and screw speed was 40 rpm with dosing speed of 15 rpm. The die was a round sheet with 4-mm-diameter holes. The extruded sample was cut and granulated in pellet form, as shown in Fig. 1(b). After extrusion, the samples were air-dried overnight, and then stored in sealed plastic bags at room temperature until further analysis. TPS was then blended with LDPE in five different levels of TPS (10, 20, 30, 40, 50 wt%). Before blending with LDPE, the thermoplastic starch was dried for 24 h at 105 °C to remove any residual water. The blends were prepared using a Brabender kneading chamber. The components were put in the chamber preheated up to 160 °C with a rotor speed of 60 rpm, and kneaded for 9 min. After homogenization, the blends were moulded in laboratory hydraulic press Fontune, Holland, at a temperature of 150 °C, pressure of 25 kPa for 5 minutes, with a preheating of 1 min. Three percentages of the SEBS-g-MA as compatibilizers were used for all ratios of LDPE/TPS blends. Fig. 2 shows the prepared LDPE/TPS blends with and without the compatibilizer. The labels of the investigated samples are LDPE/TPSX (without compatibilizer) and LDPE/TPSX/SEBS-g-MA (with compatibilizer), where X is the content of TPS in the blend (10–50 % by weight). The content of the added compatibilizer (SEBS-g-MA) was 3 wt% in all LDPE/TPSX/SEBS-g-MA blends. For example, LDPE/TPS50/SEBS-g-MA means a blend with 50wt % TPS, and 3wt % compatibilizer.

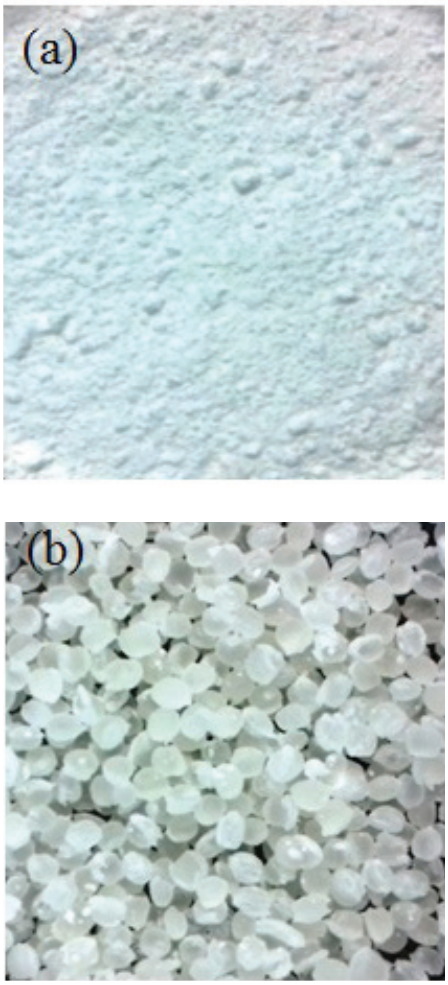

Fig. 1 – *(a) Native wheat starch in powder form, and (b) TPS (60/40 natural starch/glycerol)*

Differential scanning calorimetry (DSC)

Differential scanning calorimeter (DSC) experiments were performed using model DSC 823e (Mettler Toledo, Greifensee, Switzerland) with an intercooler cooling system in order to investigate thermal properties of the blends. Samples used for DSC measurements were weighed (around 10 mg) in aluminium pans sealed hermetically to eliminate water loss. The nitrogen flow of 60 mL min^{-1} was applied throughout the experiments. All DSC experiments were done in duplicate, and the thermograms shown refer to the second thermal scan. The tested samples were heated from ambient temperature to 150 °C at a thermal scan rate of 10 °C min^{-1}, held at 150 °C for 2 min, and after isothermal stabilization, the samples were cooled to –90 °C at the same thermal scan rate. After equilibration at –90 °C, the samples were reheated from –90 °C to 150 °C at the rate of 10 °C min^{-1}. The crystallization and melting parameters were taken from the second scans of cooling and reheating. The degree of crystallinity (χ_c) of LDPE was determined using the following equation, Eq. (1):

$$\chi_c(\%) = \frac{\Delta H_{exp}}{\Delta H_0 \cdot (1-w)} \cdot 100 \qquad (1)$$

where ΔH_{exp} is melting enthalpy (J g^{-1}) determined by DSC measurement, ΔH_0 is theoretical melting enthalpy of the completely crystalline LDPE polymer, which is 290 J $g^{-1}$and, w is mass fraction of TPS.[32]

Thermogravimetric analysis (TGA)

The thermal stability of the blends was measured by thermogravimetry using a TGA Q500 (TA Instruments, New Castle, USA). Thermogravimetric analysis was performed under a nitrogen atmosphere (60 mL min^{-1}). Samples of approximately 10 mg were heated from 25 to 700 °C at a heating rate of 10 °C min^{-1} in a nitrogen atmosphere (60 mL min^{-1}).

Scanning electron microscopy (SEM)

The morphology of the blends was characterized from the cross-sections of cryogenically fractured surfaces of the moulded bars using Vega 3 scanning electron microscope (Tescan, Brno, Czech Republic), SEM. The samples were fractured after freezing in liquid nitrogen, and the fracture surfaces were coated with gold before scanning to avoid charging under the electron beam. The electron gun voltage was set at 20 kV.

Water absorption (WA)

Water absorption (WA) of investigated blends was determined by preparing 2x2-square-inch thin film specimens using hydraulic press, Fontune, Holland, followed by hot pressing for 4 min at 160 °C and 500 kPa, cut into square specimens, and dried overnight in a vacuum oven (80 °C). Dried specimens were weighed immediately after being taken from the vacuum oven (Wi), and immersed in distilled water (23 °C, 100 % RH). After 24 h, each sample was removed from the water, lightly drained with a napkin to remove excess water on the surface of the sample, and subsequently weighed to determine its water absorption (Wa). The samples were returned in the water after each measurement. The amount of water absorbed by the samples was determined by weighing them until they were saturated and a constant weight was obtained. The percentage of water absorption at any time of each specimen was calculated by the following equation, Eq. (2):

$$\mathrm{WA} = \frac{W\mathrm{a} - W\mathrm{i}}{W\mathrm{i}} \qquad (2)$$

where Wa is the weight of the specimen at a specific time interval, and Wi is the initial dry weight of the specimen. Equilibrium moisture was assumed when the difference between successive WA values was less than 1 %.

Results and discussion

Differential scanning calorimetry (DSC)

DSC analysis was carried out to determine the effect of the additions of biodegradable thermoplastic starch, TPS, its content, and the incorporation of compatibilizer on the thermal phase transitions of LDPE and LDPE/TPS, respectively. Based on DSC curves of pure LDPE, LDPE/TPS, and LDPE/TPS/SEBS-g-MA blends, characteristic thermal phase transition parameters, such as melting temperature, T_m, melting enthalpy, ΔH_m, crystallization temperature, T_c, crystallization enthalpy, ΔH_c, and the degree of crystallinity, c_c, were determined. Thermal properties of polymers, particularly melting temperature and melting enthalpy, are influenced by thermal history applied during polymer synthesis or processing. DSC results derived from the first heating cycle give information referring to the actual state of the polymer crystals, while the cooling cycle erases the previous thermal history, such as thermal treatment during processing. Data obtained from the first heating cycle includes the effect of the prior thermal history of the extrusion process, while data obtained from the second heating cycle allows for a direct comparison of the crystallization behaviour of different materials after erasing the thermal history through the first heating cycle.[33]

As noted previously, in this study, the thermal history of the investigated materials was erased by the first scanning on DSC, and DSC curves of the second heating run by scanning from –90 to 150 °C of the investigated materials are presented. The DSC thermograms of pure LDPE and LDPE/TPS blends of cooling and second heating processes are presented in Figs. 2 and 3, and the corresponding values obtained from DSC thermograms are summarized in Table 1. Thus, these non-isothermal DSC thermograms only consist of single exothermic and endothermic peaks, which are associated with the crystal formation and melting of the crystal phase of LDPE. Specifically, all DSC data corresponds to the thermal characteristic of LDPE, since thermoplastic starch usually has no melting shape and starts to decompose before melting temperature. Melting temperatures for pure LDPE were observed between 96 °C and 121 °C, with a peak melting temperature T_m at 115 °C. The results imply a semi-crystaline structure of the LDPE. Upon cooling from 150 °C to –90 °C, crystallization of the pure LDPE occured at 98 °C. According to DSC results (Table 1), there is no significant effect of the addition of thermoplastic starch on the melting and crystallization temperature of LDPE. However, this indicated that there were no significant interactions between LDPE and TPS, suggesting immiscibility

between TPS and LDPE in LDPE/TPS blends. Incompatibility was only the consequence of the immiscibility between LDPE and TPS, due to hydrophobic character of LDPE and the hydrophilic character of TPS. Therefore, weak interface adhesion between LDPE and thermoplastic starch had occurred. On the DSC cooling curve with the main crystallization of LDPE, there is a small exothermic transition (at about 60 °C), which is related to the formation of finer LDPE crystals. This transition is also present in LDPE/TPS and LDPE/TPS/SEBS-g-MA blends.

The degree of crystallinity is one of the most important characteristics that influence physicomechanical behaviour of polymers. LDPE is a semi-crystalline polymer, and the presence of other substances and processing can induce or restrict their crystallinity. Table 1 presents the degree of crystallinity for LDPE, which was calculated using eq. (1). In general terms, the degree of crystallinity depends on the molecular architecture and thermal history of the sample.[3] In addition, the degree of crystallinity increased with increasing content of thermoplastic starch up to 20 wt% in the LDPE/TPS blends. This increase can be attributed to the favourable characteristics of glycerol of low molecular weight compared to thermoplastic starch; glycerol molecules can migrate to the surface and consequently reduce the surface tension between the components in the blend and enable better distribution of TPS phase within the LDPE matrix, which leads to the formation of good interface interactions. In addition, the increase in the degree of crystallinity can also be attributed to the nucleation effect of TPS at lower content of TPS loading in the LDPE/TPS blend. Consequently, the increase in the degree of crystallinity can be reflected in the improvement of other properties.

The morphological structure of LDPE is semi-crystalline, meaning that the LDPE crystal phase is surrounded by amorphous phase. Thermoplastic starch particles tend to position themselves in the amorphous part of LDPE. The incorporation of a higher content of TPS (> 20 wt%) leads to reduced chain flexibility of the LDPE, and thus, the degree of crystallinity of LDPE is reduced. The reason is associated with a higher content of TPS, which causes interference in the placement of polyethylene chains in more ordered structures and the formation of crystals during the cooling process.

The DSC heating curves of LDPE/TPS/SEBS-g-MA blends are shown in Fig. 4. The melting temperature of LDPE/TPS/SEBS-g-MA blends shifted to lower values in comparison to the T_m of LDPE/TPS blends. This depression in T_m is typically observed when a semi-crystalline component (LDPE) is miscible with an amorphous polymer (TPS in our case). Because the depression is moderate, the same degree of miscibility between the blend components may be concluded. In general, a decrease in melting temperature in a polymeric blend can be due to both morphological effect (decrease in lamellar thickness) and thermodynamic factors (polymer-polymer interactions).[34] From thermodynamics perspective, a decrease in melting temperature is associated with a decrease in chemical potential of the crystallisable polymer (in our case, LDPE) due to the presence of the partially miscible amorphous polymer (in our case, TPS).[23,35]

The thermal results (Table 1), suggest that SEBS-g-MA, as a compatibilizer, had a positive effect on the miscibility of the polymer in the LDPE/TPS blends. According to theory, the presence of compatibilizer contributes to the improvement of interfacial interaction at interface of the polymers, improving mutual miscibility. The crystallization temperature (Fig. 5 and Table 1) shifted to lower values with the addition of compatibilizer, indicating that the process of cooling LDPE occurred at lower temperatures. The crystallization enthalpy increased with the addition of compatibilizer to LDPE/TPS blends, suggesting the particular influence of compatibilizer on production of higher quantities of smaller crystal structures of LDPE. Also, in order to understand the influence of compatibilizer on crystallization of LDPE/TPS blends, the melting enthalpy (ΔH_m) of each blend was used to calculate the degree of crystallinity (χ_c) of LDPE in the blend (Table 1).

The degree of crystallinity of LDPE increased from around 39.3 % for neat LDPE to a maximum of 54.8 % in LDPE/TPS40/SEBS-g-MA blend. We observed that the incorporation of compatibilizer and increase in the content of TPS in LDPE/TPS blends led to a significant increase in LDPE crystallinity. This result is explained by the existence of hydrogen bonds in the starch structure, so it is stiffer and has higher crystallinity than semi-crystalline polymers, such as neat LDPE.

Thermogravimetric analysis

The thermogravimetric TG/DTG curves for native wheat starch, thermoplastic starch, and TPS with compatibilizer (TPS/SEBS-g-MA) are shown in Fig. 6. Native wheat starch shows a two-step process mechanism of decomposition. The first temperature change, observed in the temperature range of 65–120 °C, was related to the loss of adsorbed and bound water, accompanied by the formation of volatile disintegrated products**.** The thermal decomposition of starch occurred in the second step between 228–393 °C. The breakage of long chains of starch and destruction (oxidation) of the glucose rings occurred at this stage.[30,36,37] Studies on the

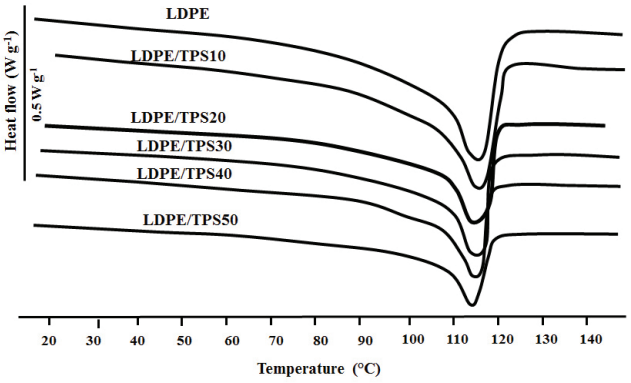

Fig. 2 – *DSC heating thermograms of LDPE/TPS blends*

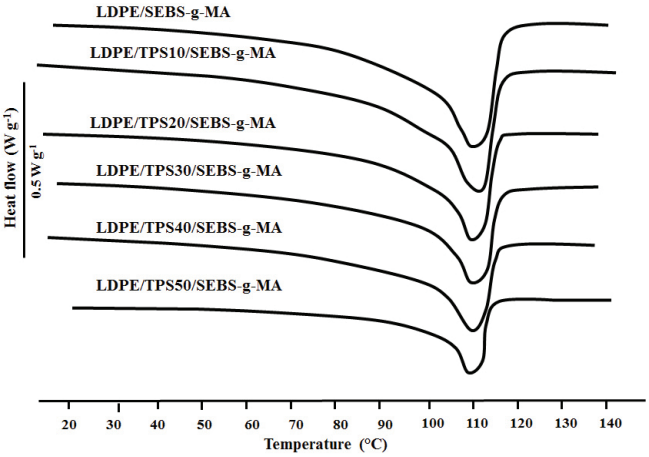

Fig. 4 – *DSC heating thermograms of LDPE/TPS/SEBS-g-MA blends*

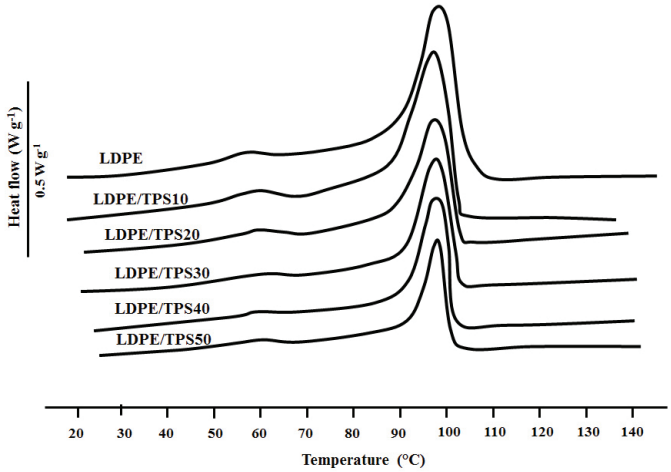

Fig. 3 – *DSC cooling thermograms of LDPE/TPS blends*

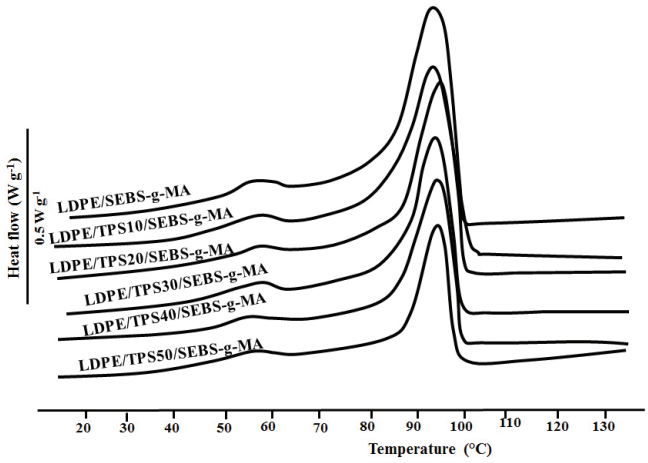

Fig. 5 – *DSC cooling thermograms of LDPE/TPS/SEBS-g-MA blends*

Table 1 – *Thermal properties of the investigated blends*

Sample	T_m, ºC	T_c, ºC	ΔH_m, J g^{-1}	ΔH_c, J g^{-1}	χ_c, %
LDPE	114.7	97.7	114.0	121.2	39.3
LDPE/SEBS-g-MA	111.7	93.9	128.5	137.1	45.7
LDPE/TPS10	114.2	97.2	105.3	120.7	40.4
LDPE/TPS10/SEBS-g-MA	112.5	93.7	128.2	133.5	50.8
LDPE/TPS20	113.7	97.3	99.2	82.2	42.7
LDPE/TPS20/SEBS-g-MA	111.8	95.0	101.0	116.0	45.2
LDPE/TPS30	114.3	97.7	74.5	69.7	36.7
LDPE/TPS30/SEBS-g-MA	112.2	94.4	98.6	109.3	50.7
LDPE/TPS40	114.2	97.5	63.1	65.6	36.3
LDPE/TPS40/SEBS-g-MA	112.2	94.4	90.6	101.3	54.8
LDPE/TPS50	113.7	98.0	48.4	46.8	33.4
LDPE/TPS50/SEBS-g-MA	111.6	94.6	63.8	64.3	46.8

T_m-melting temperature, °C; T_c-crystallization temperature, °C; ΔH_m – melting enthalpy, J g^{-1}; ΔH_c – crystallization enthalpy, J g^{-1}; χ_c – degree of crystallinity, %

thermal degradation of starch report that thermal reactions for starch start around 300 °C with thermal condensation between hydroxyl groups of starch chains to form ether segments and liberation of water molecules, and other small molecular species. Dehydration of neighbouring hydroxyl groups in the glucose ring also occurred, resulting in the formation of C=C bonds or breakdown of the glucose ring.[31,38]

On the other hand, thermoplastic starch has a clearly pronounced one-step thermal decomposition with the beginning of degradation at 160 °C, mainly assigned to the decomposition of starch with the temperature at maximum degradation rate at 332.4 °C (T_{max}). In addition, the temperature changes at about 30–130 °C are also presented and related to the evaporation of moisture contained in TPS (water and glycerol).

The results showed that the gelatization of natural wheat starch improved its thermal stability, as an extremely important property in processing and manufacturing polymers for use as packaging material. After the incorporation of SEBS-g-MA as a compatibilizer in the TPS, the onset temperature of the degradation moved to higher temperatures indicating improved thermal stability of TPS. Degradation process of TPS/SEBS-g-MA showed a two-step decomposition pattern, with onset degradation temperature at 187.9 °C, with a first maximum degradation temperature at 335.4 °C attributed to the degradation of TPS, and the second maximum degradation temperature at 490 °C attributed to the degradation of the compatibilizer (SEBS-g-MA).

As it is well known from the literature[1,39–43], under a nitrogen atmosphere, LDPE degrades in a single smooth step (Fig. 6). Thus, the beginning of LDPE degradation started at 430 °C with temperature of maximum degradation rate at 475 °C (T_{1max}) (Table 2). From the literature, the mechanism of thermal degradation of polyethylene is related to the initiation, propagation, and termination process.[44] Initiation process assumes random scission of the carbon–carbon backbone to form secondary alkyl radicals. After initiation, random abstraction of hydrogen atoms takes place by alkyl radicals. This is followed by scission of the carbon–carbon bond β to the new radical to give an allylic end group and a radical chain end as products. Termination is considered to be mainly by radical–radical disproportionation at chain ends to give a saturated and an unsaturated chain end.[43]

From the thermogravimetric results obtained for the pure LDPE compatibilized with SEBS-g-MA (LDPE/SEBS-g-MA; Fig. 3; Table 2), also thermally decomposed in a single step, degradation started at about 450 °C (at temperature of approximately 20 °C higher than pure LDPE). In addition, as may be observed from the DTG curves in Fig. 7, pure LDPE reached zero mass loss at about 495 °C. Furthermore, with the addition of compatibilizer to the pure LDPE, complete degradation occurred but with a shift of degradation temperature end to higher temperatures. The DTG curves in Fig. 7 clearly show the shift of the maximum mass loss to higher values, suggesting that compatibilizer addition to pure LDPE enhanced its thermal stability. The thermogravimetric DTG curves for LDPE/TPS blends are shown in Fig. 7, and the obtained values from the curves are summarized in Table 2.

The thermal degradation of the LDPE/TPS blends showed a two-step decomposition process (Fig. 7, Table 2). The first step of degradation at lower temperatures was related to the degradation of thermoplastic starch (T_{1max}), while the second step of degradation (above 470 °C) corresponded to the degradation of LDPE (T_{2max}). With increasing the content of TPS, LDPE degradation temperature moved to lower temperatures, contributing to the reduction in LDPE thermal stability. On the other hand, extreme thermal stability of pure LDPE contributed to increasing the thermal stability of pure TPS in LDPE/TPS blends. The thermogravimetric DTG curves of LDPE/TPS/SEBS-g-MA are shown in Fig. 8, and the TG/DTG values obtained from the curve summarized in Table 2.

The degradation of LDPE/TPS/SEBS-g-MA blends also showed two stages of degradation (Fig. 8, Table 2). The first stage of degradation at lower temperatures refered to TPS (T_{1max}) degradation,

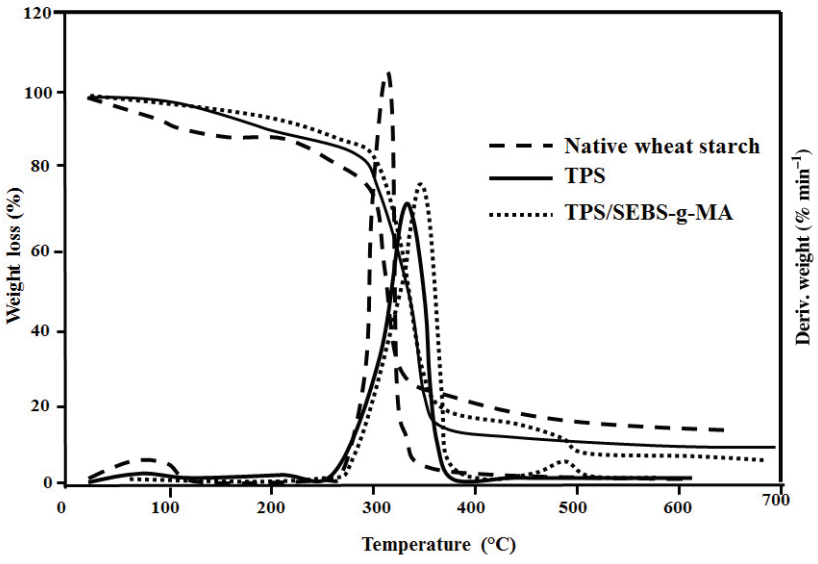

Fig. 6 – *TG/DTG curves of native wheat starch, TPS and TPS/SEBS-g-MA*

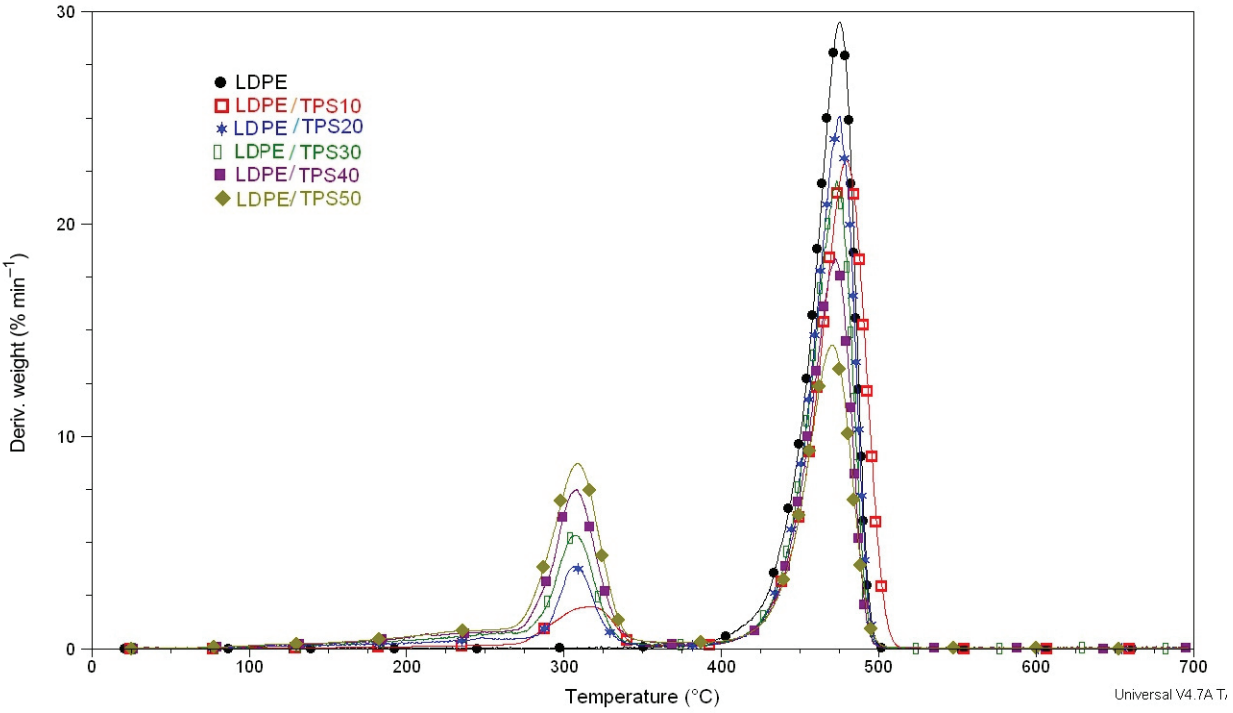

Fig. 7 – *DTG curves of LDPE/TPS*

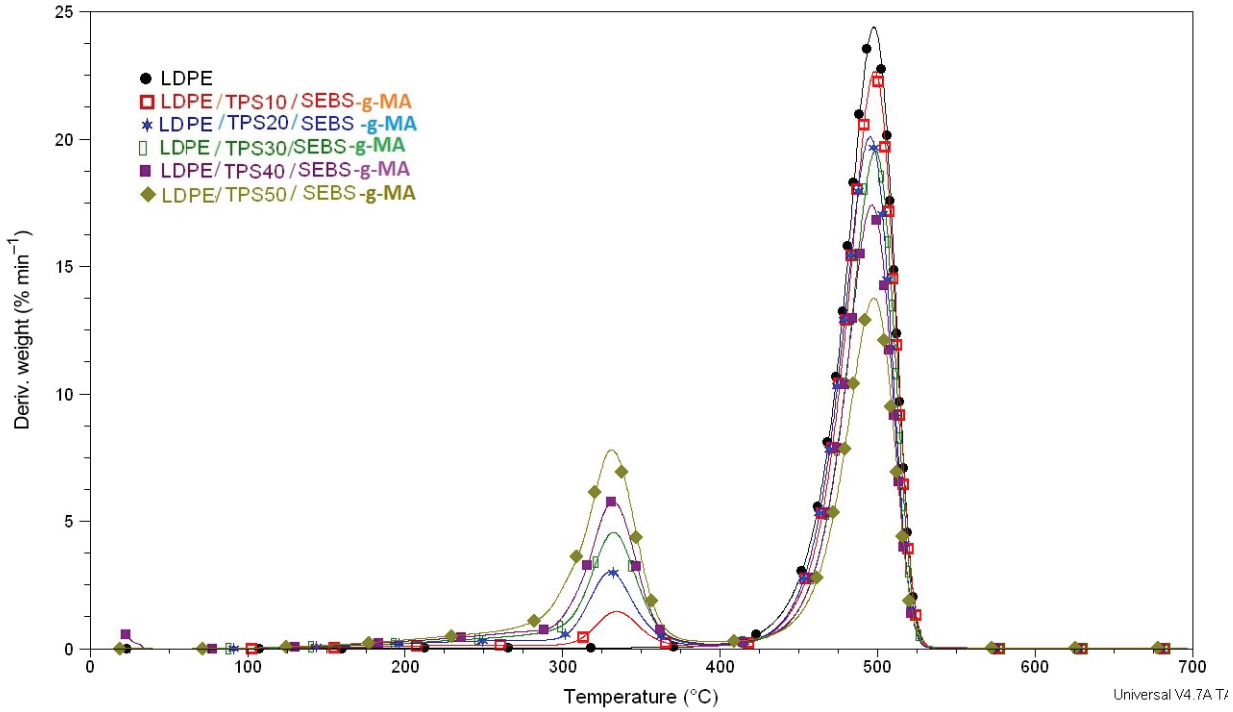

Fig. 8 – *DTG curves of LDPE/TPS/SEBS-g-MA blends*

while the second degradation step above 490 °C corresponded to the degradation of LDPE (T_{2max}). The incorporation of compatibilazer, SEBS-g-MA, the value of onset and offset degradation temperature had increased, confirming the positive effect of SEBS-g-MA on the thermal stability of LDPE/TPS/SEBS-g-MA blends. From Table 2, TG/DTG values of compatibilized blends show the decomposition point for all TPS content shifting to higher decomposition temperature when SEBS-g-MA was added as compatibilizer. The blends show slow and steady initial weight loss before first major weight loss was detected. The first degradation peak of compatibilized blends shifted by about 30–45 °C to higher

Table 2 – *Results of TGA analysis of the investigated blends*

Sample	T_{onset}, °C	$T_{1max,}$ °C	Δm_1, %	$T_{2max,}$ °C	Δm_2, %	T_{end}, °C	$R_{700\ °C}$, %
LDPE	430.1	474.7	100.0	N/A	N/A	495.3	0.0
LDPE/SEBS-g-MA	450.1	497.6	99.6	N/A	N/A	523.8	0.0
LDPE/TPS10	305.7	317.1	9.1	479.9	88.2	491.2	0.9
LDPE/TPS10/SEBS-g-MA	338.7	334.3	5.6	497.7	88.8	517.2	3.7
LDPE/TPS20	281.0	307.0	11.6	474.2	82.8	488.0	1.0
LDPE/TPS20/SEBS-g-MA	314.2	330.2	12.0	495.1	81.5	515.5	3.1
LDPE/TPS30	249.6	310.0	18.5	472.8	74.1	484.9	1.5
LDPE/TPS30/SEBS-g-MA	295.5	332.2	21.7	498.1	75.5	513.5	1.4
LDPE/TPS40	230.9	308.0	26.9	471.9	63.0	484.1	2.0
LDPE/TPS40/SEBS-g-MA	268.5	331.8	27.5	496.2	68.3	510.7	1.9
LDPE/TPS50	222.5	308.8	35.9	470.7	53.3	483.5	3.3
LDPE/TPS50/SEBS-g-MA	263.9	331.1	39.4	497.4	55.7	511.8	3.2

T_{onset} – initial degradation temperature, °C; T_{max} – temperature at maximum degradation rate, °C; Δm– weight loss, %; T_{end} – final degradation temperature, °C*;* $R_{700\ °C}$ – residue at 700 °C, %

temperatures. The second degradation peak of LDPE/TPS/SEBS-g-MA blends also showes a similar trend, which was 25–40 °C higher than uncompatibilized LDPE/TPS blends, corresponding to significant increase in thermal stability.

Scanning electron microscopy

Morphological structure of the fracture surfaces of LDPE/TPS blends with and without the addition of compatibilizer was investigated by scanning electron microscopy, SEM. From the SEM micrographs of the fracture surfaces for the initial polymer components, native wheat starch, TPS, and LDPE, were firstly analysed to determine the morphological structure in the pure polymer matrices (Fig. 9).

SEM micrographs of native wheat starch are presented in Fig. 9(a). As may be seen, the native wheat starch has a granular structure.[16] These granules are spherical or oval and have various sizes which are prone to agglomeration, similar to results found in the literature.[16] Granules are smooth, free of pores and cracks, have polyhedral shapes, flat surfaces with smooth edges, and are relatively thick. During gelatization, there occurred a transformation of granular morphology into a homogeneous polymeric film, the destruction of hydrogen bonds between the starch molecules occurred synchronously with the formation of the hydrogen bonds between the plasticizer and starch molecules, and thermoplastic starch was obtained (Fig. 9(b)). Morphology of the fracture surface of TPS was a smooth, clear, homogeneous structure, due to good dissolution of starch particles after the gelatization process.

From the SEM micrographs of the pure LDPE fracture surface (Fig. 9(d)), LDPE had a smooth surface and presented a uniform continuous matrix.[3,16,45] With the addition of SEBS-g-MA as compatibilizer to the pure LDPE (Fig. 9(e)), the smooth surface disappeared and the appearance of fibrils was observed, maybe because the hydrogenated ethylene-butadiene blocks formed entanglements with the LDPE phases. SEM micrographs of the fracture surface of uncompatibilized LDPE/TPS20 and LDPE/TPS50 blend specimens are presented in Fig. 10. Due to the large amount of results, in this paper, we present only SEM micrographs of blends with 20 wt% (lower content) and 50 wt% (higher content) of TPS, with or without compatibilizer in the LDPE matrix. The displayed SEM micrographs clearly show the difference between the higher and lower contents of the added TPS in the LDPE matrix, therefore, there was no need to display all SEM micrographs.

As may be seen from Fig. 10, the LDPE and TPS phases were incompatible; they created two-phase morphology in which the particle domains of TPS are dispersed in LDPE matrix. Within the two-phase morphology, the formation of cavities is evident, as a consequence of pulled out TPS particles, indicating weak interfacial adhesion, and high interfacial tension between the phases, due to the hydrophilic character of TPS and the hydrophobic character of LDPE. It is also visible that there are boundaries between the particles of TPS and polyethylene matrix, which indicates poor penetration of dispersed particles in the matrix due to weak adhesion at the interface. Noticeable cavities are potential places for the retention of water and accumula-

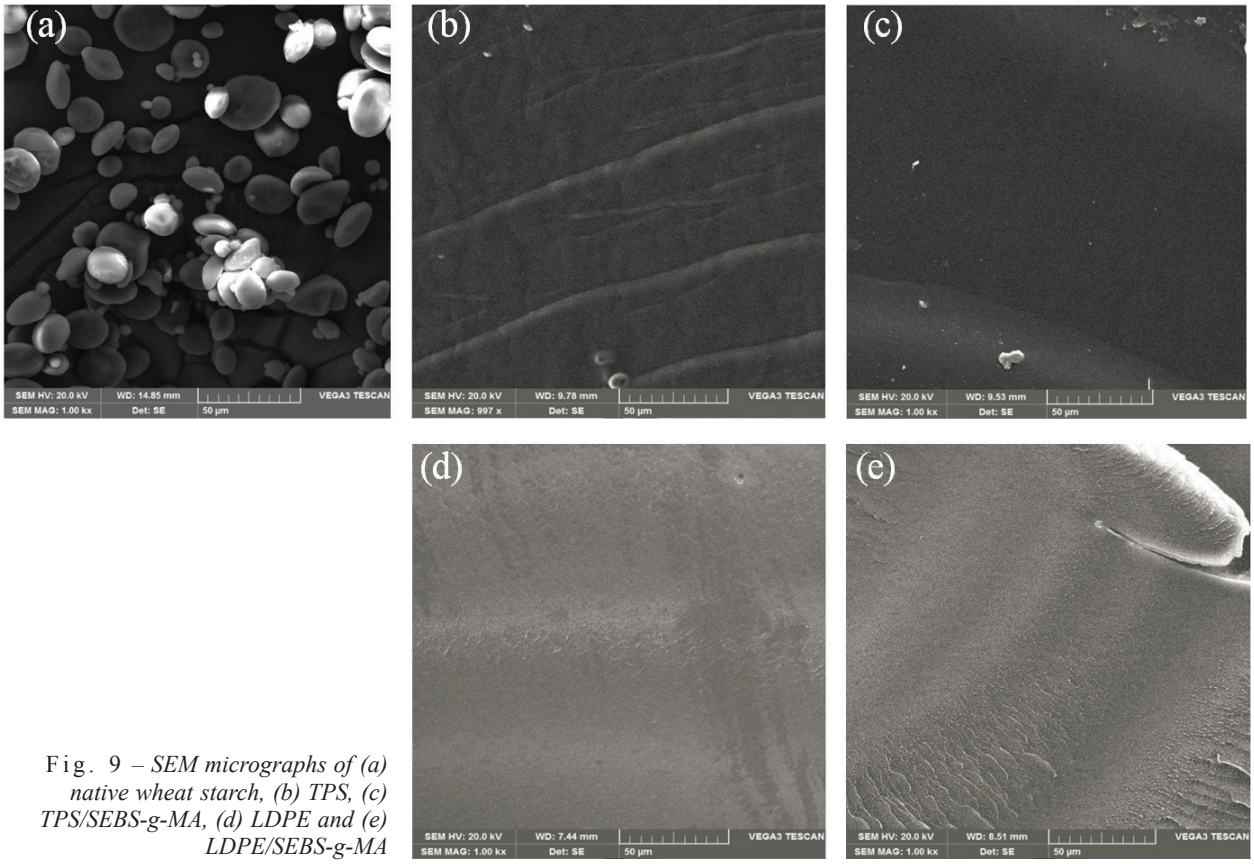

Fig. 9 – *SEM micrographs of (a) native wheat starch, (b) TPS, (c) TPS/SEBS-g-MA, (d) LDPE and (e) LDPE/SEBS-g-MA*

tion of microorganisms when such materials are used. This leads to poor stress transfer from the polymer matrix on the particles of dispersed phase, which could result in poor mechanical properties of such blends. Due to unsatisfying transfer of stress from the matrix to the dispersed particles and vice versa, cracks on the interface could occur. The higher content of TPS phase (50 wt%) (Fig. 10(c)) illustrates pronounced two-phase morphology that is more noticeable compared to the blend with lower content of TPS phase (LDPE/TPS20 blend; Fig. 10 (a)). The higher content of TPS phase in LDPE matrix led to easier coalescence of TPS particles. The particle size of the TPS phase increased in LDPE matrix, which is proportional to the content of TPS in LDPE/TPS blends. The coalescence phenomenon was responsible for increasing the particle size of TPS particles in the LDPE matrix. The coalescence, recombination of particles, respectively, took place during the blending process. The reason for that can also be linked to the difference in viscosity between the two polymer phases, and the noticeable hydrophilic/hydrophobic character.

High viscosity and hydrophobic nature of LDPE prevents diffusion of TPS domain, so it is difficult for TPS, as hydrophilic phase, to disperse throughout the LDPE matrix. Therefore, the phenomenon of coalescence becomes dominant. From the morphology point of view, the composition of the blend, as well as the processing conditions and the nature of the polymers (interfacial energy and viscosity ratio), are very important parameters. It is crucial for the coalescence phenomena of the dispersed phase to be taken into account. In fact, the final generated morphology is a balance between deformation and disintegration phenomena on one hand and coalescence on the other.

Amongst all parameters affecting morphology formation, the state of the interface is very important. In immiscible blends, the compatibility of the system can be increased using interfacial modifiers, such as block or graft copolymers, containing segments that are capable of physical and/or chemical interactions with the blend components. Compatibilized blends (Figs. 10(b) and (d)) displayed a reduced dispersed-phase size arising from coalescence suppression and interfacial tension decrease, due to the presence of interfacial modifier.

The addition of SEBS-g-MA as compatibilizer in blends might improve the interactions at the interface with polymer matrix and reinforce the system. A more homogeneous structure with less severe cavities is visible, indicating better compatibility of TPS and LDPE phases, good adhesion at the interface, respectively. The particle size of dispersed TPS particles reduced, and cavities

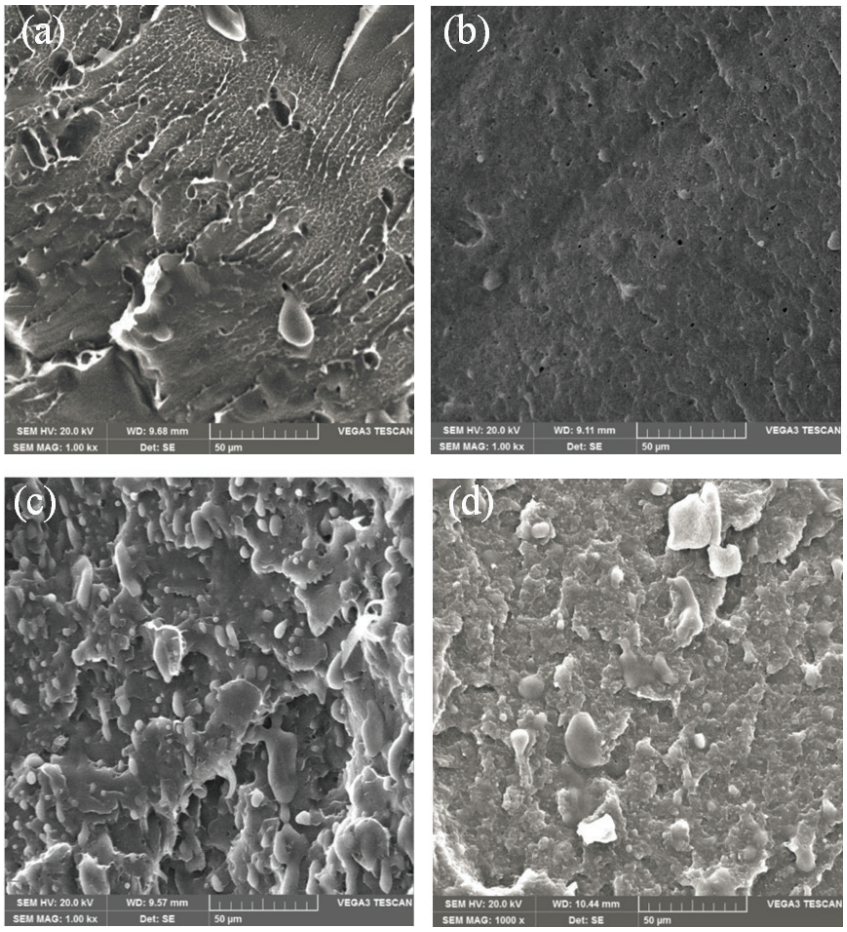

Fig. 10 – *SEM micrographs of (a) LDPE/TPS20, (b) LDPE/TPS20/SEBS-g-MA, (c) LDPE/TPS50, (d) LDPE/TPS50/SEBS-g-MA*

arising from unstable particles were less noticeable, indicating reduced interfacial tension in the presence of SEBS-g-MA as compatibilizer. The morphological structure had improved (Figs. 10(b) and (d)), more homogeneous structure was achieved, the cavity's expression was less visible, and the TPS particles were better absorbed into the LDPE matrix. The better distribution of the TPS particles throughout the polyethylene matrix was achieved; penetration of the TPS had improved, indicating the improvement of interfacial adhesion and reduction in interfacial tension with the addition of SEBS-g-MA.

The morphology of the fractured surface of the compatibilized LDPE/TPS20/SEBS-g-MA blend (Fig. 10(b)) was significantly improved in comparison with the uncompatibilized blend (LDPE/TPS20; Fig. 10(a)) of equivalent composition, with a significant decrease in the dispersed phase size, due to an increased adhesion and a lack of signs of debonding at the interface. This has been recognized elsewhere as an indication that the compatibility between phases in the blend had been improved. A higher content of TPS in the LDPE/TPS50 blend worsened the morphology of the uncompatibilized blend, but still the addition of compatibilizer lowered the domain size and displayed finer morphology (LDPE/TPS50/SEBS-g-MA). A much finer and more uniform morphology of the compatibilized LDPE/TPS20/SEBS-g-MA blend was obtained in comparison with the rough morphology of the compatibilized LDPE/TPS50/SEBS-g-MA blend.

It can be assumed that the fine and uniform dispersion of the thermoplastic starch phase in the polyethylene matrix is the result of using SEBS-g-MA block copolymer as compatibilizer. The compatibilizer reduced the interfacial tension between the hydrophilic TPS phase and hydrophobic LDPE phase, the fine dispersion of one phase into the other was achieved. The reduction of phase separation was obtained, as well as a decrease in intermediate tension, and improved interfacial adhesion, which resulted in improved processing and application properties of the final material. The excellent performance of SEBS-g-MA as compatibilizer for the LDPE/TPS blends could be linked to the ability of the grafted maleic anhydride groups to react with the hydroxyls of starch to form ester linkages; the

formation of hydrogen bonding between the hydroxyls and the carboxylic acids resulting from the hydrolysis of the anhydride.

Water absorption

Thermoplastic starch swells extremely in the presence of water, leading to a possible breakdown of the material, due to its hydroscopic nature. Starch is prone to moisture and water absorption. On the other hand, low-density polyethylene shows hydrophobic nature and high resistance to water. Therefore, water absorption as a barrier property was investigated precisely because of this difference in the highly hydrophilic character of TPS and the hydrophobic character of LDPE. It is obvious that water absorption of blends is directly proportional to the amount of thermoplastic starch incorporated into LDPE polymer matrix. In other words, water absorption would increase by increasing the starch content in LDPE.[46]

Thermoplastic starch is responsible for water absorption due to hydrophilic nature of TPS and ionic character of hydroxyl group of starch.[45] The hydroxyl group in starch can form a hydrogen bond with water, thus, it is important to investigate the water absorption properties of blends with TPS. The results of water absorption are only displayed for the LDPE/TPS blends, with and without compatibilizer (Figs. 11 and 12). Water absorption was also investigated for pure TPS and TPS/SEBS-g-MA, but was immeasurable throughout the eight days because after one hour of WA measurements, the samples were saturated and broke down, which confirmed their strong hydrophilic character. On the other hand, LDPE and LDPE/SEBS-g-MA confirmed their complete hydrophobic character (Figs. 11 and 12). Water absorption of LDPE/TPS blends was fast in the first few days, and then achieved a constant value. Water absorption of the LDPE/TPS blends increased as TPS content increased, Fig. 11. This was because starch is a hydrophilic polymer and LDPE is hydrophobic. Meanwhile, a shorter time was required to reach equilibrium at lower TPS content in the LDPE/TPS blends. On the other hand, a longer time was required to reach equilibrium at increased TPS content because the discontinuity of the LDPE matrix increased.

At high thermoplastic starch content, water could saturate the surface of the blends easily, and also penetrated into the blends through voids, and was absorbed easily by the TPS, resulting in higher water absorption in a shorter time. Fig. 11, shows that water absorption increased with both time of immersion and thermoplastic starch content. The increase in water absorption with increase in both starch content and immersion time is in agreement with previous studies on LDPE/TPS blends by other authors.[6,10–12,22,46] Furthermore, higher TPS content resulted in longer immersion time in order to achieve constant WA value. With higher starch content, water absorption is greater.

Rapid water absorption was observed for all samples during the first few days of immersion, followed by a slow increase. After 8 days, the saturation of the samples occurred and a steady state value of water absorption was achieved. For the LDPE/TPS blends with a TPS content from 10 to 30 wt%, the value of water absorption after the second day reached a constant, balanced value. The value of the water absorption of pure LDPE was 0.2 %, and with incorporation of SEBS-g-MA into the pure LDPE, the WA value increased up to 0.8 %, due to the influence of the polar maleic anhydride grafted into the structure of SEBS.

Furthermore, incorporation of the SEBS-g-MA as compatibilizer into LDPE/TPS blends contributed to the formation of a homogeneous structure with the reduction of interfacial tension between TPS and LDPE, Thus, for the application of such materials, it is extremely important to examine the water absorption. In addition, blends with higher level of water absorption have weaker mechanical properties.[45,46] In case of LDPE/TPS blends, it can be deduced that the incorporation of SEBS-g-MA as compatibilizer diminished water absorption for all LDPE/TPS blends (Fig. 12). As mentioned previously, water absorption of thermoplastic starch was very high due to the capability of water molecules to penetrate through the starch network. Further, lower water absorption of LDPE/TPS/SEBS-g-MA blends in comparison with LDPE/TPS blends was due to the role of compatibilizer, SEBS-g-MA, which reduced the water molecules' accessibility to the starch chain by blocking a tortuous pathway for water to enter the blends, because of the achieved homogeneous morphology, without cavities, as was confirmed by DSC and SEM analysis.

Conclusions

The results of this investigation established the properties of environmentally friendly materials based on low-density polyethylene (PE-LD) and thermoplastic starch (TPS) with and without the addition of block copolymers as compatibilizers.

From the SEM microphotographs, the compatibilizing effect of SEBS-g-MA block copolymer in the LDPE/TPS blends was observed; a homogeneous structure and reduction in particle size of TPS and cavities were achieved.

DSC analysis showed an increase in the degree of crystallinity at lower TPS content in LDPE/TPS blends, due to the nucleation effect of TPS and the

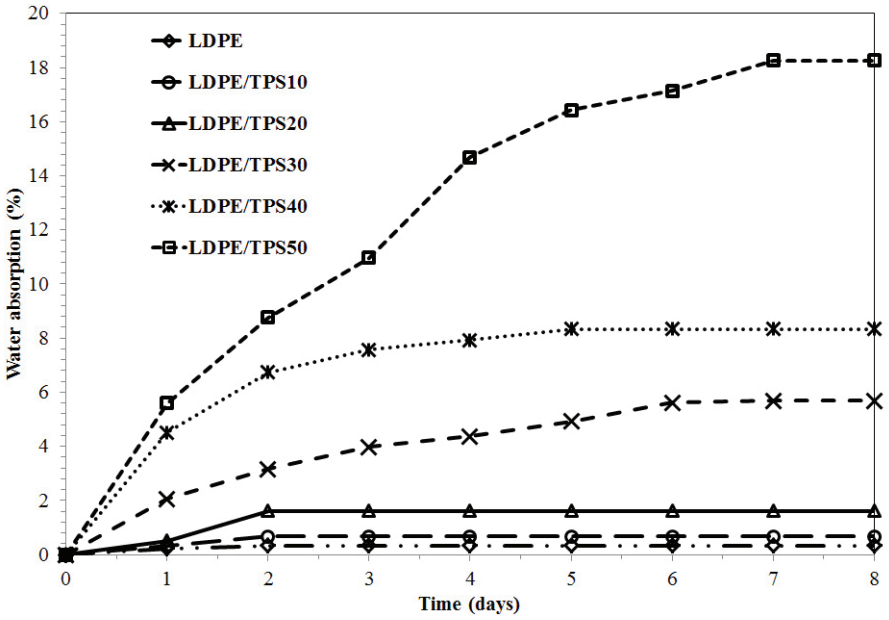

Fig. 11 – *Water absorption of the LDPE/TPS blends with immersion time*

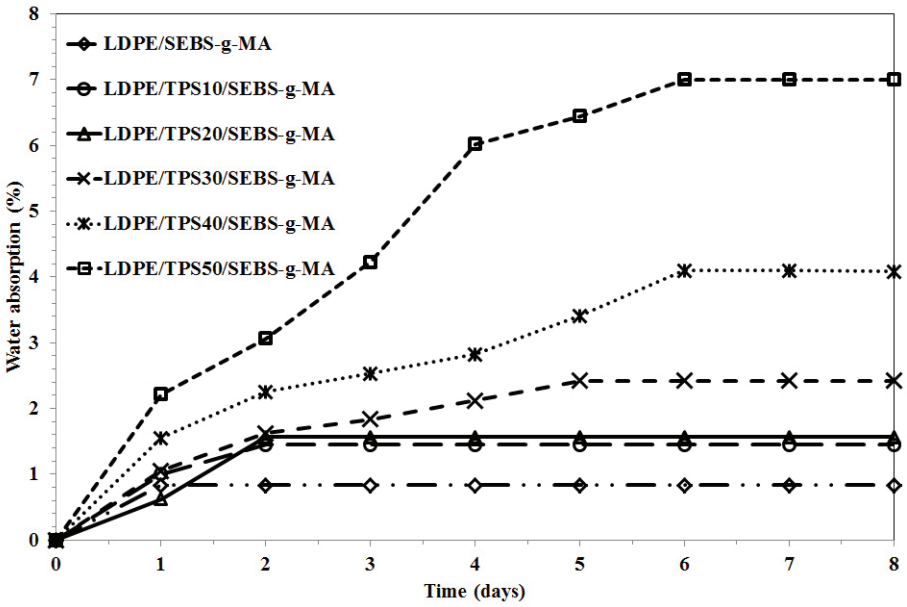

Fig. 12 – *Water absorption of the LDPE/TPS/SEBS-g-MA blends with immersion time*

possible migration of glycerol as plasticizer to the intermediate surface. With high TPS content, the degree of crystallinity decreased, due to TPS causing interference in the placement of polyethylene chains in more ordered structures and the formation of crystals during the cooling process. With the incorporation of SEBS-g-MA as compatibilizer into LDPE/TPS blends, the degree of crystallinity increased, and the melting temperature shifted to lower values, indicating the positive effect of SEBS-g-MA on the miscibility of the LDPE/TPS blends.

From TG analysis, the thermal stability of thermoplastic starch actually improved by plasticisation with glycerol, and reduction in absorbed and bound water was achieved. By adding and increasing the content of TPS, the degradation temperature shifted to a lower temperature, indicating a reduction in the thermal stability of the LDPE/TPS blends. TGA analysis showed a two-step degradation of LDPE/TPS blends, the first degradation stage related to decomposition of starch, while the second degradation stage related to the decomposition of LDPE. With the incorporation of compatibilizer, a signifi-

cant shift in the onset degradation temperature was observed, indicating an increase in thermal stability of the LDPE/TPS/SEBS-g-MA blends.

The lower water absorption of LDPE/TPS/SEBS-g-MA in comparison to LDPE/TPS may be attributed to the role of SEBS-g-MA, which was capable of reducing the water molecules' accessibility to the starch chain by blocking a tortuous pathway for water to enter the blends, owing to obtained homogeneous morphology, without cavities of LDPE/TPS/SEBS-g-MA blends, as was confirmed by DSC and SEM analysis.

However, in order to use these bio-based materials as active packaging for real food products, further research is necessary. In addition, our further research on these bio-based materials is focused on examining mechanical and other barrier properties (water vapour permeability, gas permeability). As a potential environmentally friendly material, biodegradation testing is indispensable in order to determine the degree and rate of its decomposition, which directly depends on the addition of starch to non-biodegradable LDPE, also planned in our further research.

References

1. *Siročić, A. P., Rešček, A., Ščetar, M., Krehula, LJ. K., Hrnjak-Murgic, Z.,* Development of low density polyethylene nanocomposites films for packaging, Polym. Bull. **71** (2014) 705. doi: http://doi.org/10.1007/s00289-013-1087-9
2. *Guzmán, M., Giraldo, D., Murillo, E.,* Hyper branched polyester polyol plasticized tapioca starch low density polyethylene blends, Polimeros **27** (2017) 1. doi: https://doi.org/10.1590/0104-1428.04816
3. *Vrsaljko, D., Macut, D., Kovačević, V.,* Potential role of nanofillers as compatibilizers in immiscible PLA/LDPE blends, J. Appl. Polym. Sci. **132** (2015) 41414. doi: https://doi.org/10.1002/app.41414
4. *Fortelny, I., Slouf, M., Sikora, A., Hlavata, D., Hasova, V., Mikesova, J., Jacob, C.,* The effect of the architecture and concentration of styrene-butadiene compatibilizers on the morphology of polystyrene/low-density polyethylene blends, J. Appl. Polym. Sci. **100** (2006) 2803. doi: https://doi.org/10.1002/app.23731
5. *Bonhomme, S., Cuer, A., Delort, A. M., Lemaire, J., Sancelme, M., Scott, G.,* Environmental biodegradation of polyethylene, Polym. Degrad. Stab. **81** (2003) 441. doi: https://doi.org/10.1016/S0141-3910(03)00129-0
6. *Sabetzadeh, M., Bagheri, R., Masoomi, M.,* Effect of corn starch content in thermoplastic starch/low-density polyethylene blends on their mechanical and flow properties, J. App. Polym. Sci. **126** (2012) E63. doi: https://doi.org/10.1002/app.36329
7. *Matzinos, P., Tserki, V., Gianikouris, C., Pavlidou, E., Panayiotou, C.,* Processing and characterization of LDPE/starch/PCL blends, Eur. Polym. J. **38** (2002) 1713. doi: https://doi.org/10.1016/S0014-3057(02)00061-7
8. *Kahar, A. W. M., Ismail, H., Othman, N.,* Effects of polyethylene-grafted maleic anhydride as a compatibilizer on the morphology and tensile properties of (thermoplastic tapioca starch)/ (high-density polyethylene)/(natural rubber) blends, J. Vinyl Addit. Techn. **18** (2012) 65. doi: https://doi.org/10.1002/vnl.20289
9. *Brody, A. L.,* Commercial uses of active food packaging and modified atmosphere packaging systems. In Han J. H. (Ed), Innovations in food packaging, Elsevier Science, Oxford, 2005, pp 457.
10. *Majid, R. A., Ismail, H., Taib, R. M.,* Effect of PE-g-MA on tensile properties, morphology and water absorption of LDPE/thermoplastic sago starch blends, Polym. Plast. Technol. Eng. **48** (2009) 919. doi: https://doi.org/10.1080/03602550902995018
11. *Danjaji, I. D., Nawang, R., Ishiaku, U. S., Ismail, H., MohdIshak, Z. A. M.,* Degradation studies and moisture uptake of sago-starch-filled linear low-density polyethylene composites, Polym. Test. **21** (2002) 75. doi: https://doi.org/10.1016/S0142-9418(01)00051-4
12. *Danjaji, I. D., Nawang, R., Ishiaku, U. S., Ismail, H., MohdIshak, Z. A. M.,* Sago starch-filled linear low-density polyethylene (LLDPE) films: Their mechanical properties and water absorption, J. Appl. Polym. Sci. **79** (2001) 29. doi: https://doi.org/10.1002/1097-4628(20010103)79:1<29::AID-APP40>3.0.CO;2-R
13. *Khan, B., Niazi, M. B. K., Samin, G., Jahan, Z.,* Thermoplastic starch: A possible biodegradable food packaging material—a review, J. Food Process. Eng. **40** (2017) 1. doi: https://doi.org/10.1111/jfpe.12447
14. *Ghanbarzadeh, B., Almasi*, *H.,* Biodegradable Polymers, in Chamy R. and Rosenkranz F. (Eds.), Biodegradation – Life of science, Vol. 6, InTech, Croatia, 2013, pp 141-185.
15. *Müller, M. O., Pires, A. T. N., Yamashita, F.,* Characterization of thermoplastic starch/poly(lactic acid) blends obtained by extrusion and thermopressing, J. Braz. Chem. Soc. **23** (2012) 426. doi: https://doi.org/10.1590/S0103-50532012000300008
16. *Saiah, R., Gattin. R., Sreekumar, P. A.,* Properties and biodegradation nature of thermoplastic starch, El-Soubati, A. (Ed.), Book: Thermoplastic Elastomer, InTech, Croatia, 2012, pp 57-78.
17. *Musa, M. B., Yoo, M., Kang, J. T. J., Kolawole, E. G., Ishiaku, U. S., Yakubu, M. K., Whang, D. J.,* Characterization and thermomechanical properties of thermoplastic potato starch, J. Eng. Mater. Technol. **2** (2013) 9.
18. *Antosik, A. K., Wilpiszewska, K.,* Natural composites based on polysaccharide derivatives: Preparation and physicochemical properties, Chem. Pap. **72** (2018) 3215. doi: https://doi.org/10.1007/s11696-018-0550-3
19. *Abdul, K. H. P. S., Tye, Y. Y., Saurabh, C. K., Leh, C. P., Lai, T. K., Chong, E. W. N., Fazita, N. M. R., Mohd, H. J., Banerjee, A., Syakir, M. I.,* Biodegradable polymer films from seaweed polysaccharides: A review on cellulose as a reinforcement material, eXPRESS Polym. Lett. **11** (2017) 244. doi: https://doi.org/10.3144/expresspolymlett.2017.26
20. *Neto, B. A. M., Fornari Junior, C. C. M., da Silva, E. G. P., Franco, M., Reis, N. S., Bonomo, R. C. F., de Almeida, P. F., Pontes, K. V.,* Biodegradable thermoplastic starch of peach palm (*Bactris gasipaes* kunth) fruit: Production and characterisation, Int. J. Food Prop. **20** (2017) S2429. doi: https://doi.org/10.1080/10942912.2017.1372472
21. *Imre, B., Pukánszky, B.,* Compatibilization in bio-based and biodegradable polymer blends, Eur. Polym. J. **49** (2013) 1215. doi: https://doi.org/10.1016/j.eurpolymj.2013.01.019

22. *Trommsdorff, U., Tomka, I.*, Structure of amorphous starch 2. Molecular interactions with water, Macromolecules **28** (1995) 6138.
doi: https://doi.org/10.1021/ma00122a022
23. *Li, H., Huneault, M. A.,* Comparison of sorbitol and glycerol as plasticizers for thermoplastic starch in TPS/PLA blends, J. Appl. Polym. Sci. **119** (2011) 2439.
doi: https://doi.org/10.1002/app.32956
24. *Jiang, W., Qiao, X., Sun, K.,* Mechanical and thermal properties of thermoplastic acetylated starch/poly(ethylene-co-vinyl alcohol) blends, Carbohydr. Polym. **65** (2006) 139.
doi: https://doi.org/10.1016/j.carbpol.2005.12.038
25. *Huang, M., Yu, J., Ma, X.,* Ethanolamine as a novel plasticiser for thermoplastic starch, Polym. Degrad. Stab. **90** (2005) 501.
doi: https://doi.org/10.1016/j.polymdegradstab.2005.04.005
26. *Shajaratuldur, I., Mansor, N., Zakaria, M.,* A Study on thermal behaviour of thermoplastic starch plasticized by [Emim] Ac and by [Emim] Cl, Procedia Eng. **184** (2017) 567.
doi: https://doi.org/10.1016/j.proeng.2017.04.138
27. *Ferreira, A. R. V., Alves, V. D., Coelhoso, I. M.,* Polysaccharide-based membranes in food packaging applications, Membranes (Basel) **6** (2016) 22.
doi: https://doi.org/10.3390/membranes6020022
28. *Bher, A., Auras, R., Schvezov, C. E.,* Improving the toughening in poly(lacticacid)-thermoplastic cassava starch reactive blends, J. Appl. Polym. Sci. **135** (2017) 1.
doi: https://doi.org/10.1002/app.46140
29. *Pervaiz, M., Oakley, P., Sain, M.,* Extrusion of thermoplastic starch: Effect of "Green" and common polyethylene on the hydrophobicity characteristics, Mater. Sci. Appl. **5** (2014) 845.
doi: https://doi.org/10.4236/msa.2014.512085
30. *Zhang, B., Xie, F., Zhang, T., Chen, L., Li, X., Truss, W. R., Halley, P. J., Shamshina, J. L., McNally, T., Rogers, R. D.,* Different characteristic effects of ageing on starch-based films plasticised by 1-ethyl-3-methylimidazolium acetate and by glycerol, Carbohydr. Polym. **146** (2016) 67.
doi: https://doi.org/10.1016/j.carbpol.2016.03.056
31. *Johar, N., Ahmad, I.,* Morphological, thermal, and mechanical properties of starch biocomposite films reinforced by cellulose nanocrystals from rice husks, Bio Resources. **7** (2012) 5469.
32. *Kolgjini, B., Schoukens, G., Kiekens, P.,* Three-phase characterization of uniaxially stretched linear low-density polyethylene, Int. J. Polym. Sci. (2011) Article ID 731708.
doi: https://doi.org/10.1155/2011/731708
33. *Bistričić, L., Borjanović, V., Leskovac, M., Mikac, L., McGuire, G. E., Shenderova, O., Nunn, N.,* Raman spectra, thermal and mechanical properties of poly(ethylene terephthalate) carbon-based nanocomposite films, J. Polym. Res. **22** (2015) 39.
doi: https://doi.org/10.1007/s10965-015-0680-z
34. *Mittal, V., Akhtar, T., Matsko, N.,* Mechanical, thermal, rheological and morphological properties of binary and ternary blends of PLA, TPS and PCL, Macromol. Mater. Eng. **300** (2015) 423.
doi: https://doi.org/10.1002/mame.201400332
35. *Broz, M. E., Vander, H. D. L., Washburn, N. R.,* Structure and mechanical properties of poly(d,l-lactic acid)/poly(e-caprolactone) blends, Biomaterials **24** (2003) 4181.
doi: https://doi.org/10.1016/S0142-9612(03)00314-4
36. *Glavcheva-Laleva, Kerekov, Z., Pavlov, D., Glavchev, Iv.,* Obtaining of modifiers for reduced friction by esterification of waste glycerol from biodiesel production and Sylfat 2, Chem. Sci. **3** (2015) 1.
doi: https://doi.org/10.12691/ces-3-1-1
37. *Liu, H., Xie, F., Yu, L., Chen, L., Li, L.,* Thermal processing of starch-based polymers, Progress Polym. Sci. **34** (2009) 1348.
doi: https://doi.org/10.1016/j.progpolymsci.2009.07.001
38. *Taghizadeh, M. T., Abdollahi, R.,* A kinetics study on the thermal degradation of starch/poly (vinyl alcohol) blend, Chem. Mater. Eng. **3** (2015) 73.
doi: https://doi.org/10.13189/cme.2015.030402
39. *Salvalaggio, M., Bagatin, R., Fornaroli, M., Fanutti, S., Palmery, S., Battistel, E.,* Multi-component analysis of low-density polyethylene oxidative degradation, Polym. Degrad. Stab. **91** (2006) 2775.
doi: https://doi.org/10.1016/j.polymdegradstab.2006.03.024
40. *Jakubowicz, I., Enebro, J.,* Effects of reprocessing of oxo-biodegradable and non-degradable polyethylene on the durability of recycled materials, Polym. Degrad. Stab. **97** (2012) 316.
doi: https://doi.org/10.1016/j.polymdegradstab.2011.12.011
41. *Bonhomme, S., Cuer, A., Delort, A. M., Lemaire, J., Sancelme, M., Scott, G.*, Environmental biodegradation of polyethylene, Polym. Degrad. Stab. **81** (2003) 441.
doi: https://doi.org/10.1016/S0141-3910(03)00129-0
42. *Corrales, T., Catalina, F., Peinado, C., Allen, N. S., Fontan, E.,* Photooxidative and thermal degradation of polyethylenes: Interrelationship by chemiluminescence, thermal gravimetric analysis and FTIR data, J. Photochem. Photobiol. A: Chemistry **147** (2002) 213.
doi: https://doi.org/10.1016/S1010-6030(01)00629-3
43. *Aboulkas, A., El harfi, K., El Bouadili, A.,* Thermal degradation behaviors of polyethylene and polypropylene. Part I: Pyrolysis kinetics and mechanisms, Energy Convers. Manag. **51** (2010) 1363.
doi: https://doi.org/10.1016/j.enconman.2009.12.017
44. *Audouin-Jirackova, L., Verdu, J.,* Chemiluminescence of hydrocarbon polymers, J. Polym. Sci. Part A: Polym. Chem. **25** (1987) 1205.
doi: https://doi.org/10.1002/pola.1987.080250502
45. *Anderson, T. L.,* Fracture mechanics: Fundamentals and applications, CRC Press: Taylors & Francis Group, Boca Raton, 2005, pp 258-267.
46. *Slavutsky, A. M., Bertuzzi, M. A.,* Improvement of water barrier properties of starch films by lipid nanolamination, Food Packag. Mater. **7** (2016) 41.
doi: https://doi.org/10.1016/j.fpsl.2016.01.004